DØ note 4888-Conf

# Measurement of the $t\bar{t}$ Production Cross Section in $p\bar{p}$ Collisions at $\sqrt{s} = 1.96$ TeV Using $b$-tagged Lepton+Jets Events

The DØ Collaboration
(Dated: July 22, 2005)

We present a measurement of the $t\bar{t}$ production cross section at $\sqrt{s} = 1.96$ TeV, based on the application of a lifetime-based $b$-jet identification technique to events selected in the lepton+jets channel. The data sample corresponds to an integrated luminosity of 365 pb$^{-1}$, representing a substantial increase to the data set compared to the previous version of this analysis. The preliminary result yields

$$\sigma_{t\bar{t}} = 8.1^{+1.3}_{-1.2}(stat + syst) \pm 0.5\,(lumi)\ \text{pb},$$

in good agreement with the Standard Model prediction.

*DØ Preliminary Result for Summer 2005 Conferences*

## I. INTRODUCTION

In Run I the Fermilab Tevatron delivered about 100 pb$^{-1}$ of data per experiment, which brought the discovery of the top quark [1]. With the increased statistics and collision energy of Run II, the experimental attention turned to precision measurement of top quark properties, in particular its production and decay characteristics. Theoretical calculations performed within the Standard Model predict the production cross section with an uncertainty of less than 15% [2]. Deviations from this rate would signal the presence of new physics, e.g. resonance production of $t\bar{t}$ pairs [3]. In the framework of the Standard Model, the top quark decays to a $W$ boson and $b$ quark nearly 100% of the time. Top quark pair production channels are classified according to $W$ boson decay modes. In the presented analysis, we look at the lepton+jets final state which results from the leptonic decay of one of the $W$ bosons and the hadronic decay of the other. The event signature is one lepton with high transverse momentum, large transverse energy imbalance ($\not\!\!E_T$) due to the undetected neutrino, and four jets, two of which result from hadronization of the $b$ quarks. The CDF and DØ collaborations previously reported the results of $t\bar{t}$ cross section measurement at $\sqrt{s} = 1.8$ TeV using Run I data sets [4]. Recent measurements at $\sqrt{s} = 1.96$ TeV by the CDF [5] and DØ [6, 7] collaborations agree with the SM prediction within their experimental uncertainties.

This note reports a new measurement of the $t\bar{t}$ cross section measurement in the lepton+jets channel performed using data from Run II of the Tevatron recorded by the upgraded DØ detector. The data sample corresponds to an integrated luminosity of 366 ± 24 pb$^{-1}$ in the $e$+jets and 363 ± 24 pb$^{-1}$ in the $\mu$+jets channels. The precise tracking and vertexing of the DØ detector allow to exploit the long lifetime of $b$-hadrons in order to identify $b$-jets using displaced tracks algorithms, which significantly improve the signal to background ratio.

## II. DØ DETECTOR

The Run II DØ detector is comprised of the following main components: the central tracking system, the liquid-argon/uranium calorimeter, and the muon spectrometer.

The central tracking system includes a silicon microstrip tracker (SMT) and a central fiber tracker (CFT), both located in a 2 T superconducting solenoid magnet. The SMT is designed to provide efficient tracking and vertexing capability at pseudorapidities of $|\eta| < 3$. The system has a six-barrel longitudinal structure, each with a set of four layers arranged axially around the beampipe, and interspersed with 16 radial disks. A typical pitch of 50-80 $\mu$m of the SMT strips allows a precision determination of the three-dimensional track impact parameter with respect to the primary vertex which is the key component of the lifetime based $b$-jet tagging algorithms. The CFT has eight coaxial barrels, each supporting two doublets of overlapping scintillating fibers of 0.835 mm diameter, one doublet being parallel to the collision axis, and the other alternating by $\pm 3^o$ relative to the axis [8].

The calorimeter is divided into a central section (CC) providing coverage out to $|\eta| \approx 1$, and two end calorimeters (EC) extending coverage to $|\eta| \approx 4$ all housed in separate cryostats. Scintillators placed between the CC and EC provide sampling of showers at $1.1 < |\eta| < 1.4$ [9].

The muon system, covering pseudorapidities of $|\eta| < 2$, resides beyond the calorimetry, and consists of three layers of tracking detectors and scintillating trigger counters. Moving radially outwards, the first layer is placed before the 1.8 T toroid magnets, and the two following layers are located after the magnets [10].

## III. EVENT PRESELECTION

The events under study are characterized by one high $p_T$ lepton, missing transverse energy from an undetected neutrino, two jets from hadronization of the $b$-quarks and two jets from $W$ boson decay. Additional jets are often produced by initial or final state gluon radiation. We select data samples in the electron and muon channels by requiring an isolated electron with $p_T > 20$ GeV and $|\eta| < 1.1$, or an isolated muon with $p_T > 20$ GeV and $|\eta| < 2.0$. More details on the lepton identification as well as trigger requirements are reported in [6], [7]. In both channels, we require $\not\!\!E_T$ to exceed 20 GeV and not be collinear with the lepton direction in the transverse plane. These $W$ boson candidate events must be accompanied by one or more jets with $p_T > 15$ GeV and rapidity $|y| < 2.5$ [11]. Jets are defined using a cone algorithm with radius $\Delta\mathcal{R} = 0.5$ [12]. In order to ensure statistical independence from the $t\bar{t}$ cross section measurement in the dilepton channel, events with a second high $p_T$ lepton candidate are discarded. Signal events are mostly concentrated in the third and fourth jet multiplicity bins, while the first and the second bins, dominated by $W$ boson production in association with jets, are used for a cross check of background normalization. There is still some small contamination from QCD multijet events. The fraction of such events in each jet multiplicity bin is estimated using the so-called Matrix Method [13], which relies on the fact that non-W events have smaller probability to pass tight lepton quality requirements. Table I summarizes the number of events observed in data and

TABLE I: Number of events observed after preselection in $l$+jets sample. Number of $W$-like and QCD events is estimated using Matrix Method

| | 1 jet | 2 jets | 3 jets | $\geq$ 4 jets |
|---|---|---|---|---|
| $N^{presel}_{l+jets}$ | 22769 | 8450 | 2011 | 508 |
| $N^{presel}_{(W\rightarrow l)+jets}$ | 21856.7±200.7 | 7810.2±119.0 | 1782.5±51.4 | 435.9±24.5 |
| $N^{presel}_{QCD\rightarrow l+jets}$ | 912.3±127.2 | 639.8±72.2 | 228.5±22.4 | 72.1±7.3 |

estimated number of QCD multijet and $W$-like events. At this stage $t\bar{t}$ events are considered as a part of the $W$-like event subset.

## IV. TAGGING ALGORITHM

Events from $t\bar{t}$ production contain two $b$-jets, while jets produced in association with $W$ bosons predominantly originate from light quarks or gluons. Therefore, the signal to background ratio is significantly enhanced after the requirement that at least one of the jets is $b$-tagged.

We use a secondary vertex tagging (SVT) algorithm to identify $b$-quark jets. Secondary vertices are reconstructed from two or more tracks satisfying the following requirements: $p_T > 1$ GeV, $\geq 1$ hit in the SMT layers and impact parameter significance $d_{ca}/\sigma_{d_{ca}} > 3.5$ [14]. Tracks identified as arising from $K^0_S$ or $\Lambda$ decays or from $\gamma$ conversions are not considered. If the secondary vertex reconstructed within a jet has a decay length significance $L_{xy}/\sigma_{L_{xy}} > 7$ [15], the jet is tagged as a $b$-quark jet. Events with exactly 1 ($\geq 2$) tagged jets are referred to as single-tag (double-tag) events. We treat single-tag and double-tag events separately because of their different signal-to-background ratios.

Secondary vertices with $L_{xy}/\sigma_{L_{xy}} < -7$ appear due to finite resolution of their characteristics after reconstruction, and define the "negative tagging rate". The negative tagging rate is used to estimate the probability for misidentifying a light flavor ($u$, $d$, $s$ quark or gluon) jet as a $b$-quark jet (the "mis-tagging rate").

We measure the $b$-tagging efficiency in a data sample of dijet events with enhanced heavy flavor content by requiring a jet with an associated muon at high transverse momentum relative to the jet axis. By comparing the SVT and muon-tagged jet samples, the tagging efficiency for semileptonic $b$-quark decays ("semileptonic $b$-tagging efficiency") can be inferred. We make use of a Monte Carlo simulation to further correct the measured efficiency to the tagging efficiency for inclusive $b$-quark decays. We estimate the $c$-tagging efficiency from the same simulation, corrected by a scale factor defined as the ratio of the semileptonic $b$-tagging efficiency measured in data to that measured in the simulation. We estimate the mis-tagging rate from the negative tagging rate measured in dijet events, corrected for the contribution of heavy-flavor jets and the presence of long-lived particles in light-flavor jets. Both corrections are derived from Monte Carlo.

Tagging efficiencies are parameterized as functions of jet $p_T$ and rapidity. These parameterizations are then used to predict the probability for a jet of a certain flavor to be tagged.

## V. BACKGROUND COMPOSITION

We rely on Monte Carlo to predict the flavor composition of the jets produced in association with a $W$ boson. The $W$+jets events with different jet multiplicity and flavor are generated using ALPGEN V1.3 [16] with CTEQ5L parton distribution functions [17] interfaced with PYTHIA 6.2 [18] to simulate fragmentation and underlying event and to decay all unstable particles except $B$ hadrons and $\tau$ leptons, which are modeled via EVTGEN [19] and TAUOLA [20], respectively. Events are then processed through the full DØ simulation and reconstruction. In most cases, the jets accompanying the $W$ boson originate from light ($u$, $d$, $s$) quarks and gluons ($W$+light jets). Depending on the jet multiplicity, between 2% and 14% of $W$+jets events contain heavy flavor jets resulting from gluon splitting into $b\bar{b}$ or $c\bar{c}$ ($Wb\bar{b}$ or $Wc\bar{c}$, respectively), while in about 5% of events, a single $c$ quark is present in the final state as a result of the $W$ boson radiated from an $s$ quark from the proton's or antiproton's sea ($Wc$). The number of tagged events is derived based on the number of $W$-like events observed in the data before tagging, multiplied by the fraction of a certain flavor component and the probability to tag such a combination of jets derived from Monte Carlo calibrated to reproduce data as described above.

The number of tagged QCD multijet background events in each jet multiplicity is estimated by applying the Matrix Method to the tagged preselected sample. Smaller contributions from single top, $Z$+jets, $Z \rightarrow \tau\tau$ with one of the $\tau$'s

| | $W$+1jet | $W$+2jets | $W$+3jets | $W$+$\geq$4jets |
|---|---|---|---|---|
| $W$+light | 57.1±1.1 | 32.0±1.1 | 10.2±0.5 | 2.46±0.20 |
| $Wc$ | 84.4±0.9 | 38.5±0.8 | 7.8±0.3 | 1.34±0.11 |
| $Wc\bar{c}$ | 21.5±0.2 | 28.8±0.6 | 9.73±0.3 | 3.32±0.28 |
| $Wb\bar{b}$ | 59.1±0.6 | 71.3±1.2 | 20.9±0.7 | 6.67±0.54 |
| $W$+jets | 222.0±1.6 | 170.6±1.7 | 48.6±0.8 | 13.8±0.5 |
| QCD | 18.5±2.6 | 22.8±2.9 | 10.2±1.9 | 5.4±1.5 |
| single top | 4.66±0.08 | 13.2±0.1 | 5.19±0.09 | 1.34±0.04 |
| $t\bar{t} \to ll$ | 3.11±0.05 | 12.1±0.1 | 5.9±0.1 | 1.26±0.03 |
| diboson | 3.67±0.17 | 8.29±0.27 | 1.04±0.09 | 0.08±0.02 |
| $Z \to \tau^+\tau^-$ | 1.79±0.25 | 0.86±0.16 | 0.18±0.08 | $< 0.01$ |
| background | 253.8±3.1 | 227.8±3.4 | 71.1±2.1 | 21.8±1.6 |
| syst. | +35.96-40.73 | +30.15-32.06 | +8.37-8.79 | +2.45-2.52 |
| $t\bar{t} \to l$+jets | 1.05±0.05 | 13.3±0.2 | 41.9±0.3 | 51.3±0.3 |
| total predicted. | 254.8±3.1 | 241.0±3.4 | 113.0±2.1 | 73.2±1.6 |
| syst. | +35.96-40.75 | +30.36-32.15 | +8.77-9.15 | +5.73-6.79 |
| observed | 251 | 215 | 121 | 88 |

TABLE II: Summary of observed and predicted number of $\ell$+jets events with 1 tag. Errors are statistical only.

| | $W$+2jets | $W$+3jets | $W$+$\geq$4jets |
|---|---|---|---|
| $W$+light | 0.043±0.004 | 0.028±0.003 | 0.010±0.001 |
| $Wc$ | 0.081±0.003 | 0.031±0.002 | $< 0.01$ |
| $Wc\bar{c}$ | 0.77±0.03 | 0.30±0.02 | 0.12±0.01 |
| $Wb\bar{b}$ | 10.1±0.3 | 3.25±0.14 | 1.04±0.09 |
| $W$+jets | 10.9±0.2 | 3.60±0.14 | 1.18±0.08 |
| QCD | $< 0.01$ | 0.32±0.36 | $< 0.01$ |
| single top | 1.82±0.03 | 1.00±0.02 | 0.31±0.01 |
| $t\bar{t} \to ll$ | 3.27±0.03 | 1.75±0.02 | 0.38±0.01 |
| diboson | 0.92±0.05 | 0.12±0.01 | 0.011±0.004 |
| $Z \to \tau^+\tau^-$ | 0.03±0.03 | 0.02±0.02 | $< 0.01$ |
| background | 16.9±0.3 | 6.8±0.4 | 1.88±0.38 |
| syst. | +2.81-2.79 | +1.00-0.99 | +0.31-0.31 |
| $t\bar{t} \to l$+jets | 1.70±0.04 | 10.9±0.1 | 17.4±0.1 |
| total predicted | 18.6±0.3 | 17.7±0.4 | 19.3±0.4 |
| syst. | +2.94-2.86 | +1.74-1.73 | +2.51-2.83 |
| observed | 22 | 11 | 21 |

TABLE III: Summary of observed and predicted number of $\ell$+jets events with $\geq$2 tags. Errors are statistical only.

decaying leptonically and diboson production are estimated from the calibrated Monte Carlo samples, normalized to the next-to-leading order theoretical cross sections [21, 22].

Tables II and III summarize the sample composition after tagging of $\ell$+jets events. The $t\bar{t}$ contribution is calculated assuming a $t\bar{t}$ production cross section of 7 pb. Figure 1 shows the observed and predicted number of tags for each jet multiplicity. The excess over the background in the third and fourth bins is interpreted as the $t\bar{t}$ signal. Figure 2 shows the number of tagged events in data for each jet multiplicity compared to the background and total Standard Model prediction with the systematic uncertainties.

Kinematic distributions in $\ell$+jets data with four or more jets and at least one jet tagged are compared to a sum of predicted backgrounds and $t\bar{t}$ signal in Fig. 4 in Appendix A. The plots show good agreement between the predicted and observed distributions.

## VI. $t\bar{t}$ PRODUCTION CROSS SECTION

The efficiency to tag a $t\bar{t}$ event is estimated using calibrated ALPGEN Monte Carlo sample similar to estimation of the tagging probabilities for $W$+jets events. For $t\bar{t}$ events tagging probability turns out to be somewhat higher than for the production of $W$ bosons in association with $b$-jets because $b$-jets from top quark decays are more energetic. The average probability to tag a $t\bar{t}$ event with four or more jets is measured to be 60%.

The cross section is calculated by performing a maximum likelihood fit to the observed number of events. The

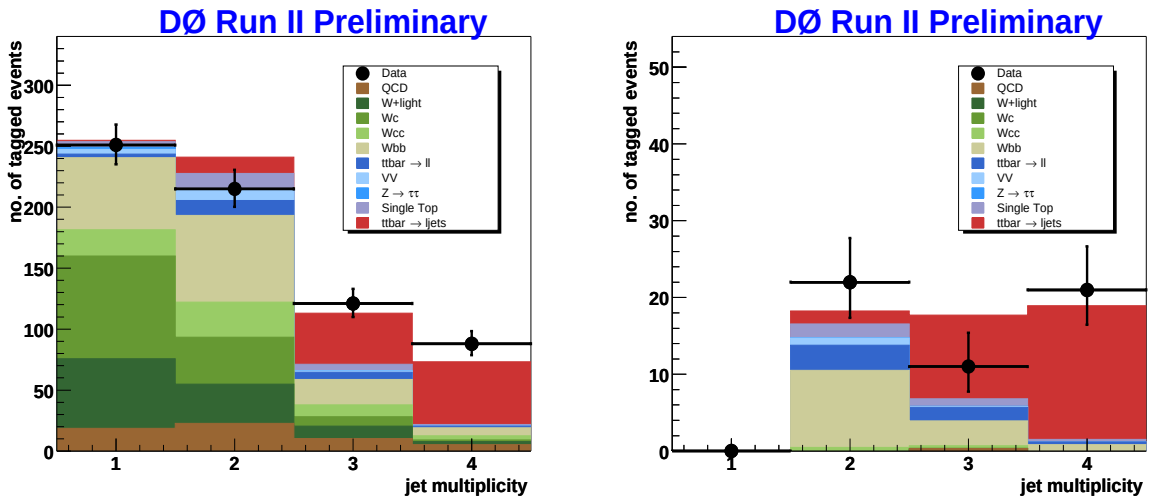


FIG. 1: Summary plot of predicted and observed tagged events in $\ell$+jets channel: single tags (left) and double tags (right).

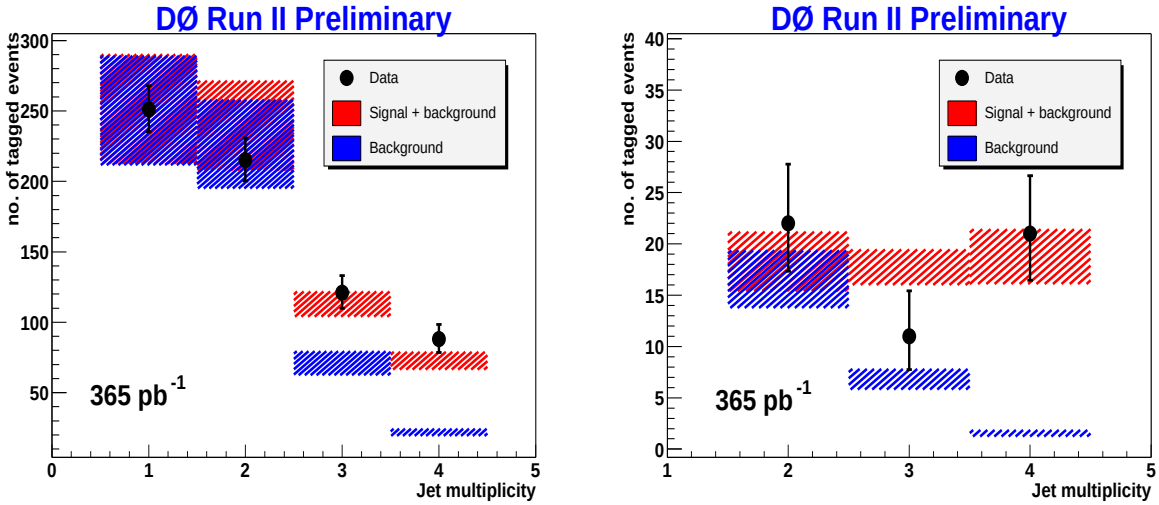


FIG. 2: Summary plot of predicted and observed tagged events in $\ell$+jets channel: single tags (left) and double tags (right) with systematic errors on the background and signal.

analysis is split into eight different channels: $\mu$+jets or $e$+jets with 3 or $\geq$4 jets and with one or two or more tagged jets. If the index $i$ refers to a channel ($\mu$+3 jets single tag, $\mu$+3 jets double tag, $\mu$+4 jets single tag or $\mu$+4 jets double tag, $e$+3 jets single tag, $e$+3 jets double tag, $e$+4 jets single tag or $e$+4 jets double tag), then the likelihood $\mathcal{L}$ to observe $N_i^{obs}$ is proportional to:

$$\mathcal{L} = \prod_i \mathcal{P}(N_i^{\rm obs}, N_i^{\rm predicted}(\sigma_{tt})) \quad (1)$$

$\mathcal{P}(N^{\rm obs}; N^{\rm predicted})$ denotes the Poisson probability to observe $N^{\rm obs}$ events when the prediction is $N^{\rm predicted}$. The predicted number of events in each channel is the sum of the predicted number of background events ($W$+jets, QCD, single top, diboson processes, $Z \to \tau\tau$) and the number of expected $t\bar{t} \to l$+jets and $t\bar{t} \to ll$ events which are functions of the $t\bar{t}$ cross section. It is assumed that the cross section is the same in the $t\bar{t} \to l$+jets and $t\bar{t} \to ll$ channels.

At each step in the maximization, the multijet background in the eight tagged samples, and the corresponding samples before tagging, is constrained within errors to the amount determined by the Matrix Method. In addition,

we include a Gaussian term for each of the systematic uncertainties considered, following the procedure described in Ref. [23]. In this approach, each source of systematic uncertainty is allowed to affect the central value of the cross section during the maximization procedure, thus yielding a combined statistical and systematic uncertainty on $\sigma_{t\bar{t}}$.

The $t\bar{t}$ production cross section for a top quark mass of 175 GeV yields:

$$\sigma_{t\bar{t}} = 8.14^{+1.27}_{-1.17}(stat + syst) \pm 0.53\,(lumi)\,\text{pb},$$

in good agreement with the previous measurement [7] based on 230 pb$^{-1}$ of data:

$$\sigma_{t\bar{t}} = 8.6^{+1.6}_{-1.5}(stat + syst) \pm 0.6\,(lumi)\,\text{pb}.$$

and the Standard Model prediction [2].

## VII. SYSTEMATIC UNCERTAINTIES

The contribution due to each individual source of systematic uncertainty can be estimated by redoing the fit after fixing all but the corresponding Gaussian term and unfolding the statistical uncertainty from the resulting total uncertainty. The statistical uncertainty of $\pm 0.9$ pb is obtained from the fit where all Gaussian terms are fixed.

The $b$-jet tagging efficiency measurement in semileptonic decays in data, the $W$ fractions and jet energy scale are the leading sources of systematics in this analysis. In addition, a systematic uncertainty of 6.5% from the luminosity measurement has been assigned. Contributions of the main sources of systematic uncertainties to the total error on the cross section are summarized in Table IV.

| Source | Offset | $\sigma^+$ | $\sigma^-$ |
|---|---|---|---|
| Muon preselections | +0.02 | +0.18 | -0.15 |
| Electron preselections | -0.02 | +0.18 | -0.15 |
| Muon triggers | +0.07 | +0.34 | -0.28 |
| Jet energy scale | -0.07 | +0.24 | -0.21 |
| Jet reco and jet ID | -0.09 | +0.23 | -0.18 |
| SML b-tag eff in MC | +0.03 | +0.15 | -0.14 |
| Semileptonic b-tagging efficiency in data | +0.18 | +0.40 | -0.35 |
| Heavy quark mass on W fractions | -0.00 | +0.18 | -0.19 |
| W fractions matching + higher order effects | +0.01 | +0.44 | -0.44 |
| Event statistics for matrix method | -0.02 | +0.15 | -0.15 |

TABLE IV: Breakdown of major sources of systematic uncertainties. For each group of systematic the likelihood maximization is redone giving a new central value of the cross section. The column labelled "offset" gives the difference between the refitted cross section and the cross section obtained in the standard method.

## VIII. CONCLUSIONS

We present a $t\bar{t}$ cross section measurement in lepton+jets final state using data from Run II of the Tevatron recorded by the upgraded DØ detector corresponding to an integrated luminosity of 365 pb$^{-1}$ which is substantially larger than the data set used for the previous measurement of the $t\bar{t}$ cross section in this channel. The Secondary Vertex Tagging algorithm is used to identify $b$-jets from top quark decay. The result

$$\sigma_{t\bar{t}} = 8.1^{+1.3}_{-1.2}(stat + syst) \pm 0.5\,(lumi)\,\text{pb}.$$

is in a good agreement with the Standard Model prediction. This result is currently the most precise $t\bar{t}$ cross section measurement at DØ as shown in Figure 3.

## IX. ACKNOWLEGEMENTS

We thank the staffs at Fermilab and collaborating institutions, and acknowledge support from the DOE and NSF (USA); CEA and CNRS/IN2P3 (France); FASI, Rosatom and RFBR (Russia); CAPES, CNPq, FAPERJ, FAPESP and FUNDUNESP (Brazil); DAE and DST (India); Colciencias (Colombia); CONACyT (Mexico); KRF

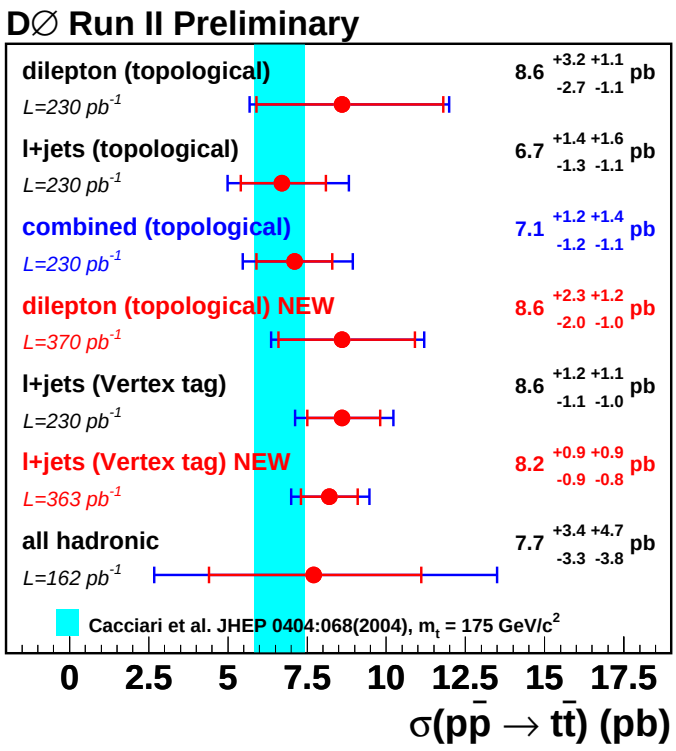


FIG. 3: Comparison of the $t\bar{t}$ cross section measurements at DØ.

(Korea); CONICET and UBACyT (Argentina); FOM (The Netherlands); PPARC (United Kingdom); MSMT (Czech Republic); CRC Program, CFI, NSERC and WestGrid Project (Canada); BMBF and DFG (Germany); SFI (Ireland); Research Corporation, Alexander von Humboldt Foundation, and the Marie Curie Program.

## APPENDIX A: KINEMATIC DISTRIBUTIONS

This section presents a comparison of some of the kinematic distributions observed in the tagged ($\geq 1$ tags) $\ell$ + jets data sample with at least four jets in the event, with the ones predicted by a sum of the background and $t\bar{t}$ signal contributions obtained from Monte Carlo weighted with the event tagging probabilities (Fig. 4). The shapes of all distributions in data are well described by the background and signal contributions, the latter is calculated assuming a $t\bar{t}$ cross section of 7 pb. The following variables are shown in the plots:

- the leading jet transverse momentum;
- the leading jet pseudorapidity;
- the $W$-boson transverse mass;
- $H_T$, the scalar sum of the $p_T$ of the four leading jets;
- the event aplanarity $\mathcal{A}$, constructed from the four-momenta of the lepton and the jets;
- the event sphericity $\mathcal{S}$, constructed from the four-momenta of the jets.

The last two variables characterize the event shape and are defined, for example, in Ref. [24].

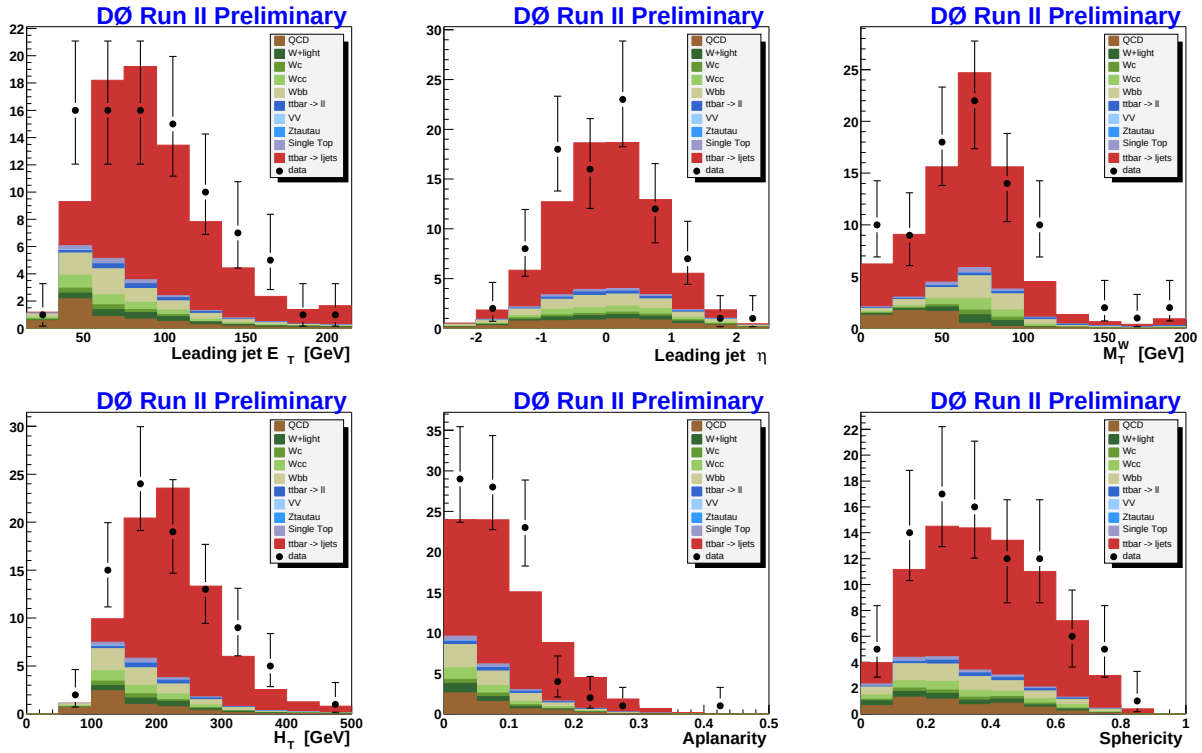


FIG. 4: Kinematic distributions for the $\ell$+$\geq$4 jets events tagged by SVT algorithm.


[1] CDF Collaboration F. Abe *et al.*, Phys. Rev. Lett. **74** 2626 (1995); DØ Collaboration, S. Abachi *et al.*, Phys. Rev. Lett. **74**, 2632 (1995).

[2] R. Bonciani, S. Catani, M.L. Mangano and P. Nason, Nucl. Phys. B **529**, 424 (1998), updated in arXiv:hep-ph/0303085; N. Kidonakis and R. Vogt, Phys. Rev. D **68**, 114014 (2003).

[3] C. T. Hill and S.J. Parke, Phys. Rev. D **49**, 4454 (1994); H.P. Nilles, Phys. Rep **110**, 1 (1984); H.E. Haber and G.L. Kane, *ibid.* **117**, 75 (1985).

[4] CDF Collaboration, T. Affolder *et al.*, Phys. Rev. D **64**, 032002 (2001); DØ Collaboration, V. Abazov *et al.*, Phys. Rev. D **67**, 012004 (2003).

[5] CDF Collaboration, D. Acosta *et al.*, Phys. Rev. Lett. **93**, 142001 (2004); CDF Collaboration, D. Acosta *et al.*, Phys. Rev. D **71**, 072005 (2005); CDF Collaboration, D. Acosta *et al.*, Phys. Rev. D **71**, 052003 (2005).

[6] DØ Collaboration, V. Abazov *et al.*, hep-ex/0504043.

[7] DØ Collaboration, V. Abazov *et al.*, hep-ex/0504058.

[8] DØ Collaboration, V. Abazov *et al.*, in preparation for submission to Nucl. Instrum. Methods Phys. Res. A;
T. LeCompte and H.T. Diehl, "The CDF and DØ Upgrades for Run II", Ann. Rev. Nucl. Part. Sci. **50**, 71 (2000).

[9] DØ Collaboration, S. Abachi *et al.*, Nucl. Instrum. Methods Phys. Res. A **338**, 185 (1994).

[10] V. Abazov *et al.*, FERMILAB-PUB-05-034-E.

[11] Rapidity $y$ and pseudorapidity $\eta$ are defined as functions of the polar angle $\theta$ and parameter $\beta$ as $y(\theta,\beta) \equiv \frac{1}{2}\ln\left[(1+\beta\cos\theta)/(1-\beta\cos\theta)\right]$ and $\eta(\theta) \equiv y(\theta,1)$, where $\beta$ is the ratio of a particle's momentum to its energy.

[12] We use the iterative, seed-based cone algorithm including midpoints, as described on p. 47 in G. C. Blazey *et al.* , in Proceedings of the Workshop: *"QCD and Weak Boson Physics in Run II",* edited by U. Baur, R. K. Ellis, and D. Zeppenfeld, FERMILAB-PUB-00-297 (2000).

[13] DØ Collaboration, S. Abachi *et al.*, FERMILAB-CONF-03-200-E.

[14] Impact parameter is defined as the distance of closest approach ($d_{ca}$) of the track to the primary vertex in the plane transverse to the beamline. Impact parameter significance is defined as $d_{ca}/\sigma_{d_{ca}}$, where $\sigma_{d_{ca}}$ is the uncertainty on $d_{ca}$.

[15] Decay length $L_{xy}$ is defined as the distance from the primary to the secondary vertex in the plane transverse to the beamline. Decay length significance is defined as $L_{xy}/\sigma_{L_{xy}}$, where $\sigma_{L_{xy}}$ is the uncertainty on $L_{xy}$.

[16] M.L. Mangano *et al.*, J. High Energy Phys. **07**, 001 (2003).

[17] H. L. Lai *et al.*, Eur. Phys. J. **C12**, 375 (2000).

[18] T. Sjostrand *et al.*, Comp. Phys. Commun. **135**, 238 (2001).

[19] D. Lange, Nucl. Instrum. Methods Phys. Res. A **462**, 152 (2001).

[20] S. Jadach *et al.*, Comp. Phys. Commun. **76**, 361 (1993).

[21] M. C. Smith and S. Willenbrock, Phys. Rev. D **54**, 6696 (1996); T. Stelzer *et al.*, Phys. Rev. D **56**, 5919 (1997).

[22] J. M. Campbell and R. K. Ellis, Phys. Rev. D **60**, 113006 (1999).

[23] P. Sinervo, in *Proceedings of Statistical methods in Particle Physics, Astrophysics, and Cosmology*, edited by L. Lyons, R. P. Mount, and R. Reitmeyer (SLAC, Stanford, 2003), p. 334.

[24] V. Barger, J. Ohnemus, and R.J.N. Phillips, Phys. Rev. D **48**, 3953 (1993).